Crystal Structure and Properties of N6/AMCC Copolymer from Theory and Fiber XRD

Youyong Li and William A. Goddard III*

Materials and Process Simulation Center (Mail Code 139-74), Division of Chemistry and Chemical Engineering, California Institute of Technology, Pasadena, California 91125

N. Sanjeeva Murthy

Physics Department, University of Vermont, Burlington, Vermont 05405

Received August 30, 2002; Revised Manuscript Received November 25, 2002

ABSTRACT: The MSXX force field developed previously from ab initio quantum calculations for studies of nylon are used to study the crystal structure and properties of the copolymer of nylon 6 with AMCC (4-aminomethylcyclohexanecarboxylic acid). For the isolated chain conformation of the copolymer, we consider both axial and equatorial connections of the chain with the cyclohexane ring and find that the best is chair-ee-St, which has equatorial connections on both ends of chair cyclohexane. We consider 12 possible crystal structures for the copolymer (the best four conformations of the isolated chain with the three forms of packing these chains: α form, γ form, and δ form). With 12.5% of AMCC in the copolymer, we find that the γ form with the chair-ee-St chain structure is the most stable, even though the α form is most stable for nylon 6. The calculated X-ray diffraction patterns of the predicted crystal structure fit both equatorial and meridional scans of XRD very well. There are two reasons that make α form less stable for the copolymer. One is the bad contact between the axial hydrogen atoms of the cyclohexane ring and the CH_2 hydrogens. The other is the difficulty of intramolecular H-bonds in the copolymer. The predicted chain-axis repeat distance of the copolymer (0 K) is 1.4 Å smaller than for the α form of Nylon 6, in good agreement with the X-ray results, which indicates that it is 1.5 Å smaller (at 300 K). Young's modulus in the chain direction is calculated to be 93 GPa for the copolymer (at 0 K), which compares to 135 and 295 GPa predicted for γ form and α form nylon 6, respectively. The introduced cyclohexane ring locates between the two amide pockets of the adjacent hydrogen bond sheets and has two major effects on the properties of the copolymer: (i) It causes twisted conformations, which decreases Young's modulus of the copolymer in chain direction. (ii) It makes the chain rigid, which likely is responsible for the decrease in sensitivity of the copolymer to moisture.

1. Introduction

Copolymers provide a robust and economical route to enhance the performance range of a polymer. "Isomorphous" replacement of ϵ-aminocaproic acid residues in nylon 6 by 4-aminomethyl-cyclohexancecarboxylic acid (AMCC) has been reported by several authors.[1−5] The nylon 6 lattice can accommodate less than 30 mol % AMCC residues before a new structure appears.[5] *cis*-AMCC isomerizes to the more thermodynamically stable trans isomer during copolymerization with caprolactam (CL) and also during homopolymerization.[5]

Nylons crystallize in two crystalline forms commonly referred to as α and γ. In the α form the hydrogen bonds are between antiparallel chains while in the γ form they are between parallel chains.[6] The α form is stable in nylon 4 while the γ form is stable for nylon 8 and above.[7] Nylon 6 is unique in that it is observed to crystallize easily in either crystalline forms and can be transformed from one to another.[8]

In this paper, we examine the effect of geometric configuration on the ability of 4-aminomethylcyclohexanecarboxylic acid (AMCC) to "isomorphously" replace ϵ-aminocaproic acid residues in nylon 6. Here we present detailed studies of the structure for the copolymer using both molecular modeling and X-ray diffraction. We conclude that just 12.5% of AMCC in the copolymer is sufficient to change the energetic preference of nylon 6 from the α form to the γ form. We will use the theory to analyze why this change occurs.

* To whom correspondence should be sent. E-mail: wag@wag.caltech.edu.

2. Calculation Details

We use the MSXX FF[7] with the MSC version of PolyGraf (version 3.30, Caltech version) for all calculations. Cerius2 (v4.0) was also used for graphics and manipulations. The electrostatic and van der Waals (vdW) interactions use the accuracy bounded convergence acceleration (ABCA) Ewald technique[9] for computing the nonbond energies of periodic systems. We use an accuracy of 0.001 kcal/mol. All structures are minimized to an rms force on all atoms of 0.01 kcal/(mol Å) for atom and rms stresses of 0.1 kcal/(mol Å) using the conjugate gradient method.

2.1. Force Field. The MSXX force field for simulation of nylon polymers was derived from ab initio QM calculations.[7] Special emphasis was given to the accuracy of the hydrogen bond potential for the amide unit and the torsional potential between the peptide and alkane fragments.

This hydrogen bond potential was derived from MP2/6-31G** calculations of the formamide dimer. Subtracting electrostatic interactions (based on fixed-point charges extracted from QC on the monomers) leads to a repulsive exponential form (eq 1) of the short-range hydrogen bond potential[7] with $A = 0.028$ kcal/mol, $C = 0.251$ Å, and $R_e = 3.017$ Å. Instead of the original charge scheme in ref 7, we now use the improved charge scheme for nylon 6 from ref 10 (see section 2.2). The difference of

10.1021/ma025635s CCC: $25.00
Published on Web 01/09/2003

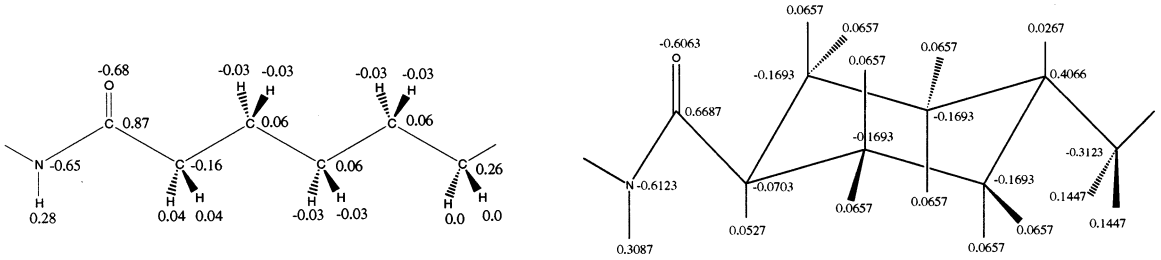

Figure 1. Charge schemes for nylon 6 monomer and AMCC monomer fragments in copolymer chain.

the two charge schemes comes from the methylene groups, which does not affect the parameters used for hydrogen bond potential.

$$E_{\mathrm{vdW}}^{\mathrm{EXP}} = A \exp\left[-\frac{(R - R_e)}{C}\right] \tag{1}$$

The full torsion potential between peptide and alkane fragment was calculated by optimizing the geometry (using HF/6-31G**) at each point on the torsional curve and the torsional potential is represented by a Fourier series (eq 2) in the MSXX force field.

$$E_{\mathrm{torsion}} = \frac{1}{2}\sum_{n=0}^{n=6} V_n \cos n\,\tau \tag{2}$$

where τ is the torsional angle ($\tau = 0$ for cis), and V_n is the barrier (energy of cis over trans).

The detailed MSXX force field was described in a previous paper.[7]

2.2. Charges. We use potential derived charges (PDQ) based on quantum mechanical calculations (HF/6-31G**) of model systems. These charges are based on calculations for long alkyl chains functionalized with an amide linkage, where a minimum of five carbons to either side was required for charge convergence.[10] On the basis of a series of calculations for shorter alkane chains functionalized with an amide, the charge perturbation within a long alkane chain due to each functional unit was extracted.[10] We use the same method to get the potential derived charges (PDQ) for AMCC monomer by fitting the total charges and the dipole moment fragment. The charge schemes for nylon 6 and AMCC are summarized in Figure 1, parts a and b.

2.3. Vibrational Calculations. The analytic second derivative matrix (Hessian) obtained directly from the complete energy expression was used to calculate the elastic constants (including Young's modulus). The methodologies are reported in refs 11 and 12 and implemented in the VIBRATE, THERMO, and ELASTICA modules in PolyGraf.

2.4. X-ray Diffraction Calculation. We use the "Diffraction-Crystal" module in Cerius2 4.0 to calculate the fiber X-ray diffraction intensities and to obtain diffraction pattern to compare with the experimental data. The intensity for each *hkl* reflection was calculated using

$$I(hkl) = \{\sum f_n \cos 2\pi\,(hx_n + ky_n + lz_n)\}^2 + \{\sum f_n \sin 2\pi\,(hx_n + ky_n + lz_n)\}^2 \tag{3}$$

where f_n is the scattering factor of atom n and x_n, y_n, z_n are the fractional coordinates of atom n. The summation is over all atoms in the unit cell.

No polarization factor, crystal monochromator factor, or temperature factor is applied to the intensity calculation.

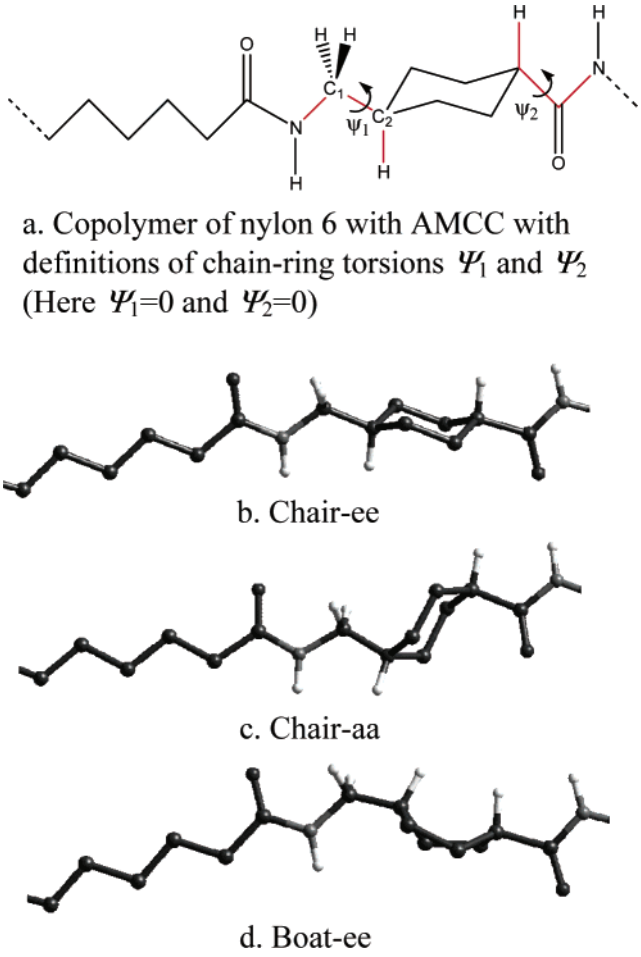

Figure 2. Three ring conformations of cyclohexane in the copolymer chain.

3. Results and Discussions

3.1. Isolated Chain Conformation of Copolymer. Before discussing the crystal structure of copolymer, we first must analyze the isolated chain conformation of the copolymer.

To maintain the roughly straight chain for the copolymer required for good crystal packing, there are three important ring conformations for the cyclohexane as shown in Figure 2b–d.

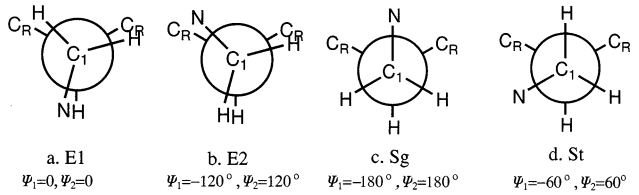

Figure 3. The four possible sets of chain-ring torsion Ψ_1 (Ψ_1 and Ψ_2 are varied simultaneously and $\Psi_1 = -\Psi_2$).

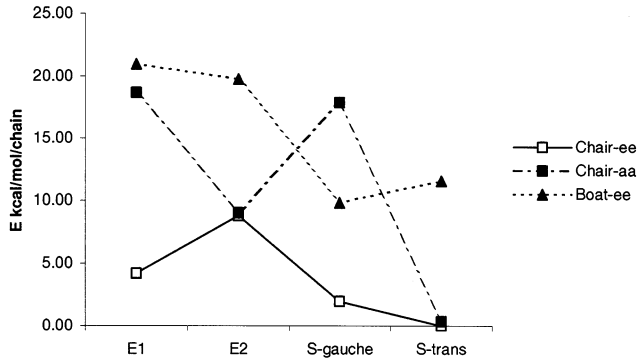

Figure 4. Relative energy of 12 isolated chain conformations.

Here, "chair-ee" is shown in Figure 2b. The cyclohexane ring of chair conformation uses two equatorial bonds to connect chain ends.

Then "chair-aa" is shown in Figure 2c. The cyclohexane ring of chair conformation uses two axial bonds to connect chain ends.

Finally, "boat-ee" is shown in Figure 2d: The cyclohexane ring of boat conformation uses two equatorial bonds to connect chain ends. The minimized structure has a twist boat conformation instead of regular boat. Twisted boat is local minimum, while regular boat is a transition state. See Figure 1.9 in ref 13.

In addition, we could construct mixed axial−equatorial structures. However all of these lead to the chains leaving the cyclohexane ring at right angles, making it less likely to pack well.

Besides the three possible ring conformations of the cyclohexane, the two bonds, which the cyclohexane ring uses to connect chain ends, may have different torsion values. Those two torsions are indicated as chain-ring torsions Ψ_1 and Ψ_2 as indicated in Figure 2a.

To keep the chain segment as shown in Figure 2 a good repeat unit, we vary the torsions Ψ_1 and Ψ_2 simultaneously. For instance, changing Ψ_1 by an angle such as +60° will make Ψ_2 changed by −60° simultaneously. Figure 3 shows the four possible chain-ring torsions of Ψ_1. "E", "S", "g", and "t" stand for "eclipsed", "staggered", "gauche", and "trans", respectively.

Combining the three ring conformation with four chain-ring torsions of Ψ_1 leads to a total 12 isolated chain conformations of copolymer.

We set the chain segment as shown in Figure 2 as a repeat unit in the unit cell and fixed the distance between two adjacent chains at 50 Å to avoid chain interactions. Torsions except Ψ_1 and Ψ_2 in the chain are fixed at 180°. Figure 4 and Table 1 show the minimized relative energy of 12 chain conformations from MSXX force field.

By analyzing the energy component, we find that the energy difference among those conformations mainly comes from the torsion part. We list the torsion part energy in Table 1.

In addition, the repulsion between axial groups of cyclohexane decreases the stability of isolated chain. The repulsion in chair-aa-Sg becomes significant, making its energy to high by 17.89 kcal/mol.

We find that with the chains attached energy difference between chair and twisted boat is 9.82 (kcal/mol)/chain (see Table 1), which is bigger than the value of 6.9 kcal/mol for cyclohexane.[14] This increase arises from steric interactions of the substituted groups, which is consistent with the conclusion in ref 13.

The chain-axis repeat distance of 12 isolated chain conformations are listed in Table 1. Here, chair-ee-E1 has the longest chain and similar chain shape as full-extended chain in α form of nylon 6. Then, chair-aa-Sg has the shortest chain, and it causes the great repulsion among axial groups.

In conclusion, the four best conformations among all 12 possibilities of isolated chain are chair-ee-St, chair-ee-Sg, chair-aa-St, and chair-ee-E1. Although chair-ee-E1 is not energy favorable compared with the other three, it keeps the longest chain and is most compatible with the full-extended nylon 6 chains. We will consider it in the following discussion. Those four conformations of copolymer chain and their relative energies are shown in Figure 5.

3.2. Crystal Structure of Copolymer from Molecular Modeling. The single bond torsion potentials, C−C(amide) torsion Φ_1 and N(amide)−C torsion Φ_2 as defined in Figure 6, are particularly important for nylon. The primary difference between the α form and γ form of nylon 6 comes from these two dihedrals. We did a systematic study[8] of crystal structures of Nylon 6 before this study of copolymer and we found three types of regular crystal structures: α form, γ form, and δ form. Similarly as the study of nylon 6, we denote the definitions of α form, γ form, and δ form of copolymer as follows: α form, $\Phi_1 \approx \Phi_2 \approx \pm 166°$, and hydrogen bonds are formed between antiparallel chains; γ form, $\Phi_1 \approx \Phi_2 \approx \pm 127°$, and hydrogen bonds are formed between parallel chains; δ form, $\Phi_1 \approx \Phi_2 \approx \pm 166°$, and hydrogen bonds are formed between parallel chains.

The Φ_1 and Φ_2 of the same chain have opposite signs (e.g., $\Phi_1 \approx +127°$, $\Phi_2 \approx -127°$) to keep the straight chain.

One copolymer chain of two amide units as shown in Figure 5 and three chains of nylon 6 are used to construct crystal structure of copolymer, whose mole fraction is 12.5%. We will consider α form, γ form, and δ form together with four conformations of copolymer chain as shown in Figure 5. There are in total 12 possible crystal structures.

Unlike nylon 6 homopolymer, whose hydrogen bond sheet can slide easily over the adjacent sheet,[8] the hydrogen bond sheet in copolymer cannot slide due to the large size of cyclohexane ring. As shown in Figure 12, the cyclohexane ring requires significant space and wants to be adjacent to the amide unit of the adjacent hydrogen bond sheet. (See the amide pocket model in ref 8.) The favored energy is about 0.8 kcal/mol/(amide unit) to fit the cyclohexane ring in the amide pocket of adjacent hydrogen-bond sheet.

For the three crystal forms (α,γ,δ) with four chain conformations (chair-ee-E1, chair-ee-St, chair-ee-Sg, chair-aa-St), Figure 7 and Table 2 show the relative energy of 12 crystal structures. The chain-axis repeat distances are listed in Table 2.

Table 1. Relative Total Energy *E*, Torsion Energy $E_{torsion}$ [(kcal/mol)/chain], and Chain-Axis Repeat Distance *b* (Å) of All 12 Possible Isolated Chain Conformations (Three Ring Conformations with Four Ring−Chain Torsions)[a]

	E1			E2			Sg			St		
	E	$E_{torsion}$	*b*	*E*	$E_{torsion}$	*b*	*E*	$E_{torsion}$	*b*	*E*	$E_{torsion}$	*b*
chair-ee	*4.18*	*3.52*	*17.0*	8.79	7.72	16.5	*1.97*	*2.92*	*16.0*	***0.00***	***0.00***	***16.5***
chair-aa	18.66	7.63	16.2	9.01	4.61	16.6	17.89	4.43	14.1	***0.32***	***1.34***	***16.1***
boat-ee	20.96	16.59	16.6	19.77	13.28	16.6	**9.82**	**7.07**	**16.5**	11.53	8.13	16.9

[a] For each ring conformation, the best ring-chain torsion is shown in boldface. In italics, we show the four best conformations among all 12 possibilities, which we will analyze in the periodic case.

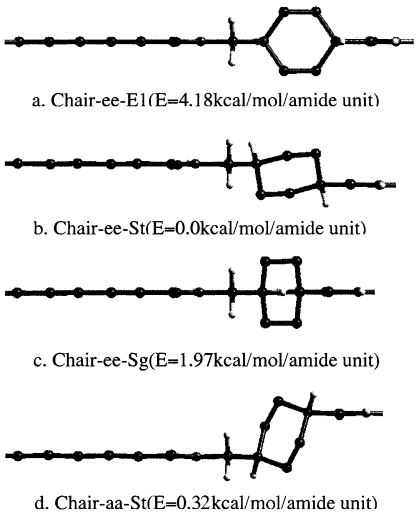

Figure 5. The four best chain conformations of the N6/AMCC copolymer.

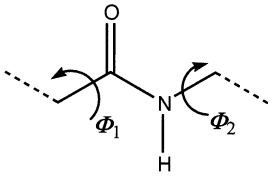

Figure 6. Definitions of amide torsion parameters: torsion Φ_1 [C−C(amide)] and torsion Φ_2 [N(amide)−C].

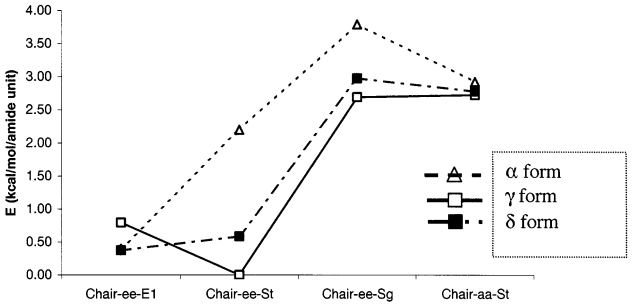

Figure 7. Relative energy [(kcal/mol)/amide unit] of the 12 crystal structures. For the three crystal forms (α,γ,δ) with four chain conformations (chair-ee-E1, chair-ee-St, chair-ee-Sg, chair-aa-St).

In general, the α form is worse than the δ form and the δ form is slightly worse than the γ form. The reasons are discussed in section 3.5.

The relative packing energies of chair-ee-St, chair-aa-St, and chair-ee-Sg have the same trend as for the isolated chain conformations. However, the unstable isolated chain conformation chair-ee-E1 has a good packing energy relative to other isolated chain conformations. As mentioned previously, chair-ee-E1 leads to the longest chain conformation with a chain shape similar to the full-extended chain of nylon 6 and hence is anticipated to be most compatible in a nylon 6 matrix.

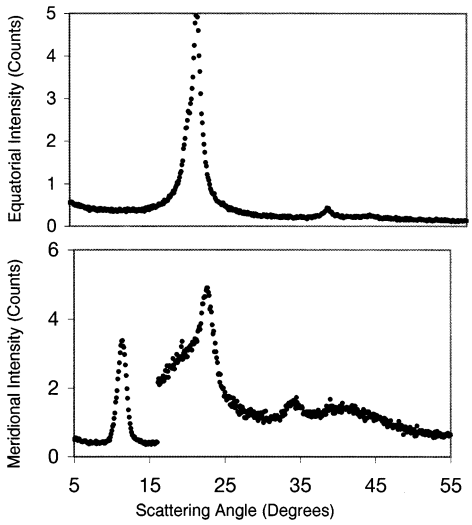

Figure 8. Experimental equatorial and meridional XRD scans of copolymer fiber.

In conclusion, the isolated chain conformation of chair-ee-St is the best (see section 3.1), and the γ form of chair-ee-St is the best crystal structure for the copolymer.

3.3. Crystal Structure of Copolymer from XRD. Figure 8 shows XRD scans from drawn/heat-set (annealed) fibers from the copolymer. The equatorial scan of the copolymer fiber is typical of the γ crystalline form. For nylon 6, the unit cells of the α and γ forms are different, and therefore the equatorial reflections of the α and γ forms appear at slightly different angles. The two intense reflections of the α and γ forms are at 21° (200, α_1) and 24° (002 + 202, α_2) and at 22° (100, γ_1) and 23° (201 + 200, γ_2), respectively.[15] See XRD scans of nylon 6 in Figure 2 in ref 15. The equatorial scans of the undrawn fibers of N6 homopolymer and N6/AMCC copolymer are quite similar,[16] indicative of the presence of γ form in both the fibers. While N6 transforms into the α form upon heat-setting, the copolymer remains in the γ form,[16] which is consistent with the molecular modeling result. A detailed discussion is given in part 3.5.

The meridional scan of the copolymer fiber is similar to the N6 homopolymer. (Compare Figure 8 with Figure 2 in ref 15.) The significant difference is that the (0*k*0) reflections show clearly that the chain-axis repeat is shorter in the copolymer than in N6. The chain-axis repeat distance is 15.7 Å in the copolymer compared to 17.2 Å for α and 16.8 Å for the γ crystalline forms of nylon 6. See part 3.6 for further discussion.

3.4. Calculated X-ray Diffraction Patterns. From the results in section 3.2, the best crystal structure is the γ form of chair-ee-St. The second best is the δ form of chair-ee-E1, while the third is the α form of chair-ee-E1 and the fourth is the δ form of chair-ee-St. These four best structures include the best structure in each

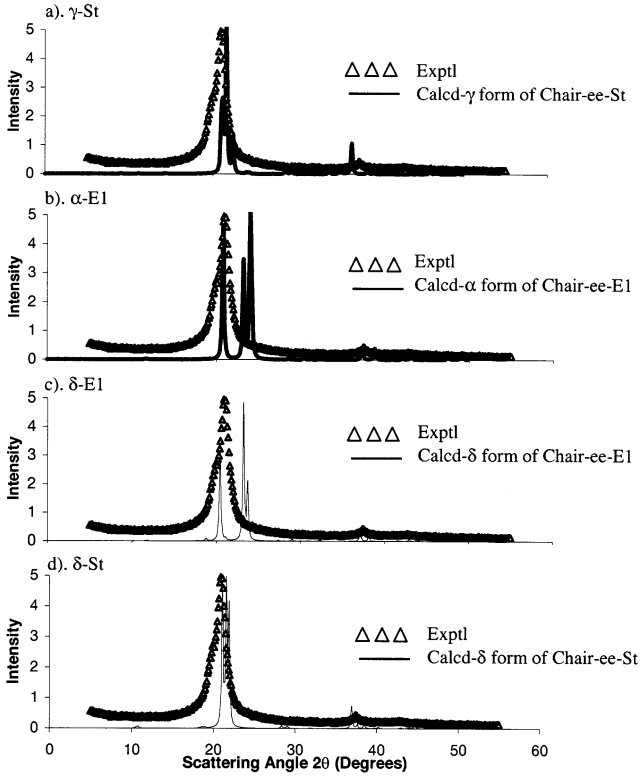

Figure 9. Calculated equatorial scan of 12.5% N6/AMCC copolymer compared with experimental equatorial scan of 10% N6/AMCC annealed fiber: (a) calculated γ form of chair-ee-St; (b) calculated α form of chair-ee-E1; (c) calculated δ form of chair-ee-E1; (d) calculated δ form of chair-ee-St (only γ-St and δ-St fit the experimental equatorial scan pattern).

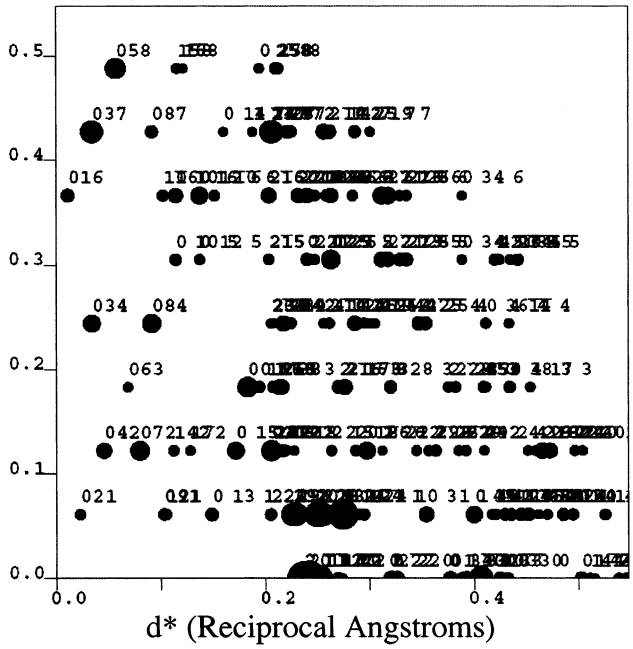

Figure 10. Quadrant precession diffraction pattern of the γ form of chair-ee-St calculated from Cerius2. The intensities are indexed from the reindexed unit cell shown in Figure 12.

of the α, γ, and δ forms. We calculated the X-ray diffraction patterns of these four structures to compare with the experimental diffraction patterns.

Figure 9 shows the calculated X-ray diffraction patterns of equatorial scan for these four structures of 12.5% N6/AMCC copolymer. (Note that the maximum intensity of the calculated pattern has been rescaled to be the same as the experimental one. See part 2.4 for calculation details.) The calculated equatorial scan of γ form chair-ee-St and δ form chair-ee-St both fit the observed fiber XRD equatorial scan well, while the chair-ee-E1 α form differs significantly. Indeed, the equatorial scans from the α and γ forms of N6/AMCC copolymer are similar to those from the α and γ forms of homopolymer nylon 6. (Compare Figure 9 with Figure 2 in ref 15.)

The equatorial scan does not distinguish between the γ form chair-ee-St and the δ form chair-ee-St. Both have

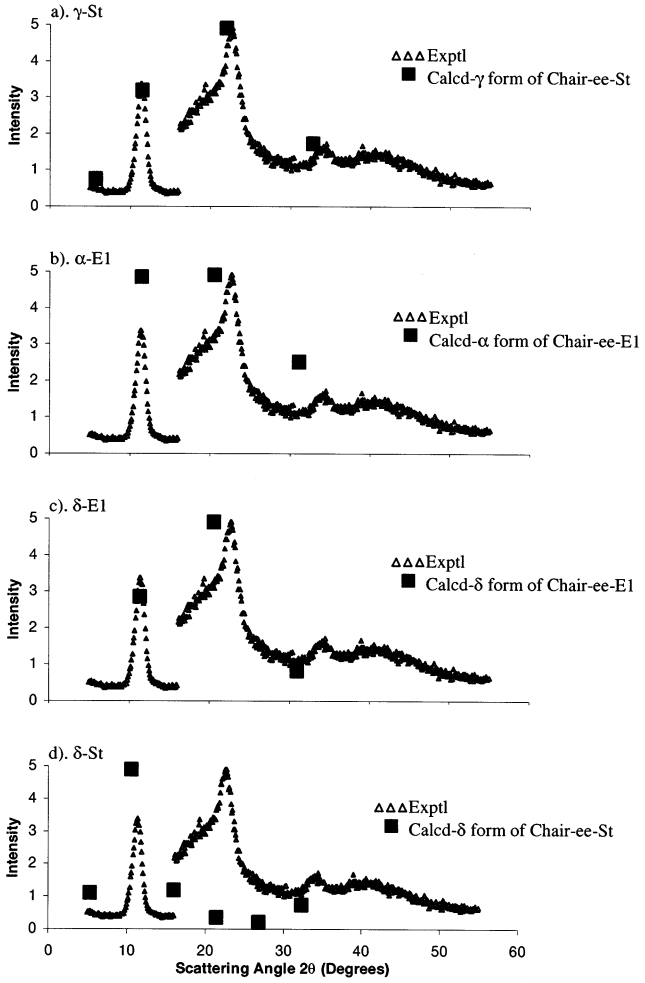

Figure 11. Calculated meridional intensities of 12.5% N6/AMCC copolymer Compared with experimental equatorial scan of 10% N6/AMCC annealed fiber: (a) calculated γ form of chair-ee-St; (b) calculated α form of chair-ee-E1; (c) calculated δ form of chair-ee-E1; (d) calculated δ form of chair-ee-St (only the γ form of chair-ee-St gives meridional intensities that fit the XRD pattern).

Table 2. Relative Energy *E* [(kcal/mol)/amide unit], Young's Modulus in Chain Direction E_Y (GPa), and Chain-Axis Repeat Distance *b* (Å) of the Three Types of Crystal Structures (α, γ, δ) Formed by Four Chain Conformations (chair-ee-E1, chair-ee-St, chair-ee-Sg, chair-aa-St)[a]

	α form			γ form			δ form		
	E	E_Y	*b*	*E*	E_Y	*b*	*E*	E_Y	*b*
chair-ee-E1	**0.40**	**237.85**	**17.4**	0.79	73.03	16.9	**0.37**	**165.20**	**17.4**
chair-ee-St	2.20	123.43	16.9	**0.00**	**92.74**	**16.3**	0.58	50.48	16.6
chair-ee-Sg	3.79	50.49	16.3	2.69	29.01	15.8	2.98	34.02	16.2
chair-aa-St	2.93	84.79	16.3	2.73	128.69	16.2	2.78	105.73	16.3

[a] The best one for each type (α, γ, δ) is shown in boldface.

similar equatorial scans as the experimental diffraction pattern. Consequently, we calculate the meridional scan for those structures to make further comparison with experiment. For ideally oriented fibers in which the *c** axis coincides with the fiber axis, the reciprocal-lattice points with indices (00*l*) (for monoclinic unit cell) cannot intersect the sphere of reflection. Thus, no reflections appear on the meridian of the diffraction pattern unless the fiber is somewhat inclined with respect to the direct beam. However, Buerger-type precession cameras have the advantage of including the meridional reflections, which in principle are not accessible to the stationary flat-film techniques. Consequently, we calculate the precession pattern instead of the stationary flat-film pattern.

Figure 10 shows the quadrant precession diffraction pattern of the γ form of chair-ee-St calculated from Cerius2. Figure 10 shows that the absolute meridional scan from precession pattern is still zero. The calculated precession patterns of the other three structures, which are not shown here, are similar, and the absolute meridional scans are zero. The reason is that our minimized crystal structures are triclinic instead of monoclinic. There are 44 chains in the re-indexed monoclinic unit cell (see Figure 12) and they neutralize the intensities (00*l*) to zero. In the experiment, the actual fibers frequently possess a sufficiently wide spread of orientations about the ideal fiber axis to generate meridional reflections. From this point, we estimate a toleration of 0.05 $Å^{-1}$ along equatorial direction, and we assume that the diffraction intensities inside 0 $\pm$ 0.05 $Å^{-1}$ along equatorial direction are observable in the experimental meridional scan. In this way, we get the "meridional" intensities of these four structures as shown in Figure 11. (The maximum intensity of calculated has been rescaled to experiment as in Figure 9.)

From Figure 11, we see that only the γ form of chair-ee-St fits the experimental meridional scan. Thus, although the calculated equatorial scan of δ form of chair-ee-St fits the experimental equatorial scan very well, its calculated meridional intensities differ from the experimental meridional scan significantly.

In conclusion, by comparing the calculated equatorial scan and meridional intensities of the best four candidate structures, the γ form of chair-ee-St, the α form of chair-ee-E1, the δ form of chair-ee-E1, and the δ form of chair-ee-St, we find that only the γ form of chair-ee-St fits the experimental patterns very well, while the other three differ substantially. This confirms our calculated energy results in part 3.2.

3.5. Relative Stability of Different Crystalline Forms of Copolymer. The homopolymer of nylon 6 can be produced either in the α form, in a mixture of α and γ crystalline forms, or in the γ form depending on the spin/draw conditions.[15] In contrast, the copolymer exists only in the γ form, and retains the short chain-axis repeat distance of this γ form even after annealing in an autoclave.[16] IR spectra confirm that conformation in the copolymer in the copolymer is the same as that in the γ form in the N6 homopolymer.[16]

For the copolymer of N6/AMCC, the α crystalline form is not favorable, even though it is the most favorable for the nylon 6 homopolymer. There are two reasons:

1. In the α form, the hydrogen bonds are in the plane of the *trans*-alkane segment. The hydrogen bonds in the α form are formed between antiparallel chains (Figure 13a). In the γ and the δ forms, the hydrogen bonds are formed between parallel chains (Figure 13b). As discussed in part 3.6 of ref 8, unlike in the γ and δ forms, there are unfavorable contacts between the hydrogen atoms in the α form of N6. This situation is worsened for the copolymer because of the large size of the cyclohexane ring; the hydrogen atoms on the cyclohexane ring are in contact with the CH2 atoms on the adjacent chains, and this is not desirable. From Figure 12, parts a and c, we can see that the cyclohexane ring in γ form of chair-ee-St locates between two amide pockets (see ref 8 for definition) avoiding the bad hydrogen contacts.

2. Intramolecular H-bonds are hard to form due to the large loop strain of the copolymer chain.

We consider a covalently connected polymer chain as one molecule.[8] As discussed in section 3.4 of ref 8, for the α form, hydrogen bonds are formed *intra*molecularly, while in γ or δ forms, they are formed *inter*molecularly. *intra*molecular H-bonds in the α form are entropically favored and dynamically favored from solution.[8] Assuming 90% hydrogen bonds are formed in amorphous region and most of them are *inter*molecular H-bonds, the γ form is kinetically favored from the melt. Annealing the γ form of nylon 6 transfers it to the thermostable α form with *intra*molecular H-bonds. Thus, as-spun fibers of N6 are in the γ form, while drawn/heat-set (annealed) fibers are in the α form.[15,16]

There is a ring constraint in the loop part of intramolecular H-bonds, while there is not such a ring constraint in intermolecular H-bonds.[8] This competing factor favors intermolecular H-bonds in nylon 6 and becomes more significant in the N6/AMCC copolymer due to the rigidity of copolymer chain.

The thermal characteristics and the effect of moisture[16] on the copolymer suggests that the copolymer chain is *more* rigid than the N6 homopolymer chain. It is easy to understand that a cyclohexane ring is more rigid than pentamethylene. Thus, in the copolymer, intramolecular H-bonds are much harder to form due to large loop strain of the copolymer and rigidity of cyclohexane than N6 homopolymer, which makes the α form of copolymer unfavorable.

3.6. Short Repeat Distance for Copolymer. The chain-axis repeat of the copolymer is found to be 15.7 Å from fiber X-ray diffraction (see Figure 8), the shortest ever observed for nylon 6. The reported chain-axis repeats for the α and γ forms and the complex of iodine/N6 are 17.2, 16.8, and 15.8−16.0 Å, respectively.[16,17] This short repeat is observed at comonomer concentration as low as 10−15 mol %.

On the basis of the results of parts 3.1 and 3.2, we attribute this unusual short chain-axis repeat distance to the twisted chain conformation of copolymer. The best isolated chain conformation of copolymer is chair-ee-St, which is *not* fully extended (due to the eclipsed bonds of the cyclohexane and the adjacent chain) as shown in Figure 5b. In addition, the torsions Ψ_1 and Ψ_2 are twisted and packed as γ form (see part 3.2). As shown in Figure 12, the N6 chains adjacent to the cyclohexane ring adjust their shapes to get good packing energy.

We calculate (0 K) a chain-axis repeat distance of 16.3 Å for the best structure, γ form of chair-ee-St of copolymer, which is 1.4 Å shorter than our calculation for the α form of N6 and 1.0 Å shorter than our calculation for the γ form of N6. From Table 3, we see that chain-axis repeat distance of copolymer from fiber X-ray is 1.5 Å shorter than the experimental α form of

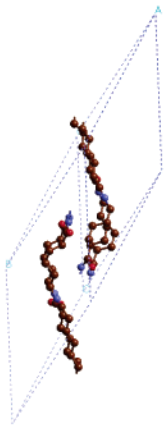

12*a*. Original triclinic unit cell projected in H-bond direction

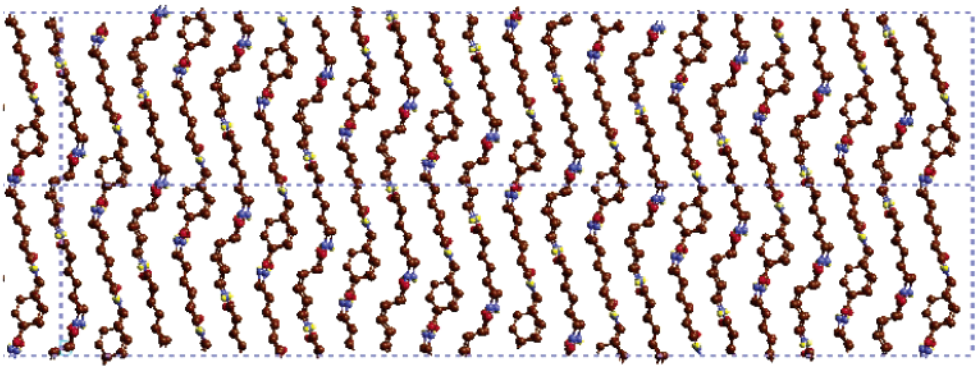

12*c*. Reindexed monoclinic unit cell projected in H-bond direction

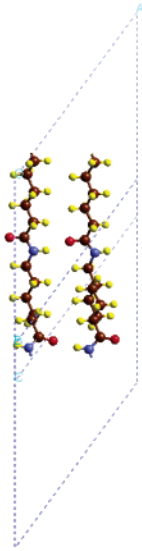

12*b*. One H-bond sheet in the original triclinic unit cell

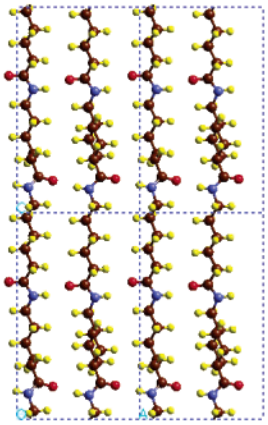

12*d*. One H-bond sheet in the reindexed monoclinic unit cell

Figure 12. Crystal structure of the γ form of chair-ee-St (parts a and b are visualizations of the original triclinic unit cell, whose cell parameters are $a = 18.25$ Å, $b = 15.56$ Å, $c = 16.37$ Å, $\alpha = 30.57°$, $\beta = 136.88°$, $\gamma = 147.50°$; parts c and d are visualizations of the re-indexed monoclinic unit cell, whose cell parameters are $a = 9.81$ Å, $b = 87.12$ Å, $c = 16.37$ Å, $\gamma = 88.80°$) (see comment in ref 18).

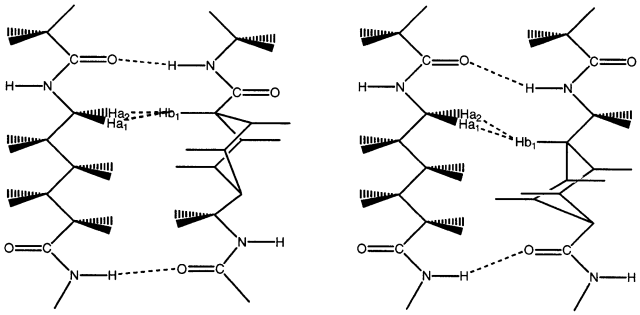

a. H-bond between antiparallel chains

b. H-bond between parallel chains

Figure 13. Hydrogen bonds between antiparallel chains or parallel chains.

N6 and 1.1 Å shorter than the experimental γ form of N6. There exist systematic differences between the experimental chain-axis repeat distance from XRD (300 K) and the theoretical value (0 K). This systematic difference arises from disorder in the chain conformations at room temperature (experiment) compared to the 0 K of theory. The fact that the actual fibers frequently possess a sufficiently wide spread of orientations about the ideal fiber axis will also decrease the observed chain repeat distance from the meridional scan of XRD. In addition, imperfections and folding in the crystal experiment will generally decrease the chain-axis repeat distance. Table 3 shows that the chain-axis repeat distance from theory is consistent with experimental result.

Table 3. Young's Modulus in Chain Direction E_Y (GPa) and Chain-Axis Repeat Distance b (Å) of the Nylon 6 α Form and γ Form and the Copolymer from Theory (γ Form of chair-ee-St) and Experiment

	nylon 6 α form		nylon 6 γ form		N6/AMCC	
	E_Y	b	E_Y	b	E_Y	b
expt	168	17.2		16.8		15.7
theory	295	17.7	135	17.3	93	16.3

3.7. Young's Modulus for Copolymer. Young's modulus in the chain direction is evaluated by the

method described in part 2.3. The results are listed in Table 2. Young's modulus of the best structure, the γ form of chair-ee-St is calculated to be 93 GPa, which is lower than the α form and the γ form of the N6 homopolymer (295 and 135 GPa, respectively[8]). As discussed in parts 3.1, 3.2, and 3.6, there is a slight twist in the chain to accommodate the eclipsing of CH bonds, which gives the chains in the copolymer a slightly unextended character. This twisted chain conformation decreases Young's modulus of the copolymer in chain direction.

This is considerable less for the α,δ forms of N6/AMCC copolymer. We note that the chain axis repeat for α,δ are 7% longer than for γ. Thus, extending the chains in the chain direction by tension might stabilize α,δ. However, as discussed in part 3.5 and ref 8, the loops in the α form are not comparable as in γ and δ and the situation is worsen when cyclohexane is introduced. This suggests that the $\gamma \rightarrow \alpha$ transition of copolymer is harder than of pure nylon 6.

The introduction of the AMCC core into the nylon 6 matrix leads directly to two results:

The chain conformation in the favorable packing structure becomes twisted instead of straight, which decreases Young's modulus of the copolymer in chain direction.

It makes the chain rigid, which likely is responsible for the decrease in sensitivity of the copolymer to moisture. Thus, the wet modulus of the copolymer is higher than that of the homopolymer, even though dry modulus of the copolymer is a little lower than the homopolymer. (See Table 1 in ref 16.)

4. Summary

The MSXX force field developed previously from ab initio quantum calculations for studying nylon is used here in conjunction with and X-ray diffraction to determine the crystal structure of copolymer of nylon 6 with AMCC (4-aminomethylcyclohexanecarboxylic acid).

We calculate the 12 crystal structures formed from all 4 plausible isolated chain conformations of copolymer with the three packing forms observed in nylon (γ, α, and δ). We predict (Figure 7) that the best structure is the γ form of chair-ee-St, which has the chains equatorial to chair cyclohexane. Bad contacts between the axial hydrogen atoms of the cyclohexane and the CH_2 of the nylon 6 on adjacent chains together with the difficulty of intramolecular H-bonds in the copolymer make the α form unfavorable. Indeed, this prediction is confirmed by the fiber X-ray diffraction experiment, which is in good agreement with the predicted patterns (Figures 9 and 11).

We predict that the stable structure (γ form of chair-ee-St) of AMCC/N6 copolymer has a chain repeat distance 1.4 Å shorter than the predicted distance of α form of nylon 6. This is conformed by the experiments, which give the difference 1.5 Å between AMCC (15.7 Å) and nylon 6 α form (17.2 Å). The twisted chain conformation caused by torsion Ψ_1,Ψ_2, Φ_1, and Φ_2 accounts for the decrease in the chain repeat distance.

Young's modulus in the chain direction is calculated to be 93 GPa for the copolymer (at 0 K), which compares to 135 and 295 GPa for the γ form and the α form of nylon 6, respectively.

The introduction of cyclohexane into nylon 6 has two major effects to its properties:

It causes twisted conformations, which decreases Young's modulus of the copolymer in the chain direction.

It makes the chain rigid, which decrease the sensitivity of the copolymer to the moisture.

Acknowledgment. This research was partially supported by grants from NSF (CHE99-85574), DOE ASCI ASAP, and ARO-MURI. The facilities of the MSC are also supported by grants from DOE, NSF (CHE 99-77872), ARO (MURI), ARO (DURIP), IBM-SUR, NIH, ChevronTexaco, 3M, Seiko-Epson, Avery-Dennison, General Motors, Kellogg's, Asahi Chemical, Beckman Institute, and Nippon Steel.

References and Notes

(1) Pietrusza, E. W.; Nesty, G. A.; Pinter, R. U.S. Pat. 3,037,-002, 1962.
(2) Levine, M.; Temin, S. C. *J. Polym. Sci.* **1961**, *49*, 241.
(3) Bogdanov, M. N.; Kudryavtsev, G. I.; Mandrosova, F. M.; Spirina, I. A.; Ostromogol'skii, D. E. *Vysokomol. Soedin.* **1961**, *3*, 1326.
(4) Temin, S. C.; Levin, M. U.S. Patent 2,910,457.
(5) Prince, F. R.; Pearce, E. M.; Fredericks, R. J. *J. Polym. Sci.: Part A-1* **1970**, *8*, 3533−3541.
(6) Kohan, M. I. *Nylon Plastics Handbook*; Hanser: New York, 1995.
(7) Dasgupta, S.; Hammond, W. B.; Goddard, W. A., III. *J. Am. Chem. Soc.* **1996**, *118*, 12291.
(8) Li, Y.; Goddard, W. A., III *Macromolecules* **2002**, *35*, 8440.
(9) Karasawa, N.; Goddard, W. A., III *J. Phys. Chem.* **1989**, *93*, 7320.
(10) Dasgupta, S.; Brameld, K. A.; Fan, C.-F.; Goddard, W. A., III. *Spectrochim. Acta Part A* **1997**, *53*, 1347.
(11) Karasawa, N.; S. D.; Goddard, W. A., III. *J. Phys. Chem.* **1991**, *95*, 2261.
(12) Karasawa, N.; Goddard, W. A., III *Macromolecules* **1992**, *25*, 7268.
(13) Juaristi, E. *Conformational behavior of six-membered rings*; VCH Publishers: New York, 1995.
(14) Dixon, D. A.; Komornicki, A. *J. Phys. Chem.* **1990**, *94*, 5630.
(15) Murthy, N. S. *Polym. Commun.* **1991**, *32*, 301.
(16) Murthy, N. S.; Cooke, R. S.; Bray, R. G. *Macromolecules*, Submitted for publication.
(17) Murthy, N. S. *Macromolecules* **1987**, *20*, 309.
(18) We clarify the source of the calculated meridional and equatorial intensities (to specify the value of *hkl*) by re-indexing the unit cell. The original minimized unit cell is triclinic as shown in Figure 12a,b. To facilitate the analysis, we re-index the unit cell as shown in Figure 12c,d. The monoclinic unit cell shown in Figure 12c,d is 11 times the original unit cell shown in Figure 12a,b in the *b* direction (*b* is the stacking direction of H-bond sheets, the *a* direction is the H-bond direction, and the *c* direction is the chain direction). The intensities shown in Figure 10 are indexed from the monoclinic unit cell. A careful study of Figure 10 reveals that we do *not* include (037) and (058) intensities in Figure 11a. The reason is that the copolymer we studied using theory assumes that cyclohexane ring is distributed uniformly in the matrix, while in the experimental study, the cyclohexane ring is distributed randomly in the matrix. Thus the intensities (037) of the 7th layer and (058) of the 8th layer would like to be negligible in the XRD meridional scan, and these layers are relatively strong in our calculated meridional intensities. From our re-indexed values of *hkl*, we can understand why the intensities inside the region of 0 ± 0.05 Å^{-1} along the equatorial direction are observed in the meridional scan. All these intensities have $h = 0$ and k as a small number. Because the monoclinic unit cell is 11 times the original unit cell and the *b* length of the re-indexed unit cell is 87.1 Å, so it is reasonable that 0*kl* intensities are in approximately the direction of 00*l*.

MA025635S